Fluorescence Control on Panchromatic Spectra via C−Alkylation on Arylated Quinoxalines

ARTICLE *in* THE JOURNAL OF ORGANIC CHEMISTRY · MAY 2009

Impact Factor: 4.72 · DOI: 10.1021/jo9002147 · Source: PubMed

7 AUTHORS, INCLUDING:

Ho-Jin Son
Korea University, Sejong, Korea
38 PUBLICATIONS **701** CITATIONS
SEE PROFILE

Won-Sik Han
Seoul Women's University
55 PUBLICATIONS **744** CITATIONS
SEE PROFILE

JOC Note

Fluorescence Control on Panchromatic Spectra via C-Alkylation on Arylated Quinoxalines

Ho-Jin Son, Won-Sik Han, Dae-Hwan Yoo, Kyoung-Tae Min, Soon-Nam Kwon, Jaejung Ko,* and Sang Ook Kang*

Department of Materials Chemistry, Sejong Campus, Korea University, Chung-Nam 339-700, South Korea

sangok@korea.ac.kr

Received February 3, 2009

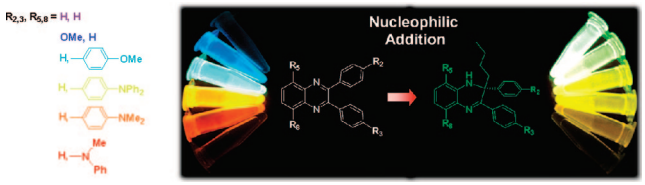

A coherent green fluorescence was obtained by butylation at the 2-position of panchromatic 2,3-diaryl-5,8-diarylquinoxalines (**2**) to give corresponding 2-butyl-2,3-diaryl-5,8-diaryl-1*H*-quinoxalines (**3**). Full color quinoxaline derivatives (**2**) were prepared from electronic modification at either the 2,3- or 5,8-positions at the peripheral ArX group or X group (X = −H, −OMe, $-NPh_2$, $-NMe_2$, −NMePh) of the quinoxalines. 2-Butylation converted one imine unit of the pyrazine ring to an amine group, which effectively altered the electron donor and acceptor functions to produce a coherent green fluorescence.

Color control and high luminescence efficiency are fundamental issues in the development of full-color emitting materials for OLEDs. Several conditions are essential for the development of new types of highly luminescent materials. These include easy preparation, facile derivatization, photochemical and thermal stability, and, most of all, color purity and high quantum efficiency.[1,2] Quinoxaline derivatives, which are known as "benzopyrazine", have a synthetic advantage over other fused aromatic systems due to the existence of a high-yield synthetic route from diketone and diamine condensation.[3] In addition, the introduction of internal diimine units to the aromatic ring system allows electronic alterations to impart highly electrophilic characteristics to the ring.[4] As a consequence, benzopyrazines are finding increasing use in light-emitting[5] and electron-transporting[6] materials for the manufacture of highly efficient OLEDs. In this study, the embodiment of full color fluorescence was achieved through the modification of quinoxalines using existing synthetic protocol and the electrophilic nature of the pyrazine ring. In addition, subsequent color control to a mostly "green" luminescence was demonstrated. A synthetic strategy for the production of highly fluorescent materials based on quinoxalines involves the introduction of electron donor (ED) substituents at the periphery of an electron-deficient quinoxaline core. New types of bipolar quinoxalines were produced by combining with an electron-withdrawing (EW) pyrazine core to yield panchromatic fluorescence depending on the electron donating capability of the ArX or X substituent. Further electronic control is expected by derivatization on this unit due to the highly polarized nature of the imine unit of the pyrazine ring.[7]

In this study, unique C-alkylation on various types of quinoxaline derivatives, **2**, consolidated their electronic structures to produce green fluorescence. Therefore, in an effort to gain further insight into the unique electronic control by C-alkylation, quinoxaline derivatives (**2**) with a full color range of 400−641 nm were prepared by 2,3-/5,8-ArylX or X substitution (X = −H, −OMe, $-NPh_2$, $-NMe_2$, −NMePh). As expected, C-alkylation on the quinoxaline precursors with *n*-butyllithium resulted in a coherent fluorescence at approximately 550 nm in all 2-butylated products (**3**). This paper reports full details of the synthesis and characterization of various 2-butylated quinoxaline compounds (**3**). Ultraviolet/visible and photoluminescence spectroscopy were used to characterize corresponding photoluminescence properties, and the direct band gaps were measured by cyclic voltammetry. Theoretical calculations were also carried out to account for the change in the electronic structures arising from the 2-butylation of quinoxaline derivatives. Using a literature protocol,[8] 5,8-dibromoquinoxaline (**1**) was prepared in moderate yield from 3,6-dibromobenzene-1,2-diamines and benzils. Schemes 1 and

(1) (a) Li, Z.; Meng, H. *Organic Light-Emitting Materials and Devices*; CRC Press: Boca Raton, FL, 2007. (b) Shirota, Y.; Kageyama, H. *Chem. Rev.* **2007**, *107*, 953.

(2) (a) Forrest, S. R.; Thompson, M. E. *Chem. Rev.* **2007**, *107*, 923. (b) Kafafi, Z. H. *Organic Electroluminescence*; Taylor & Francis: Boca Raton, FL, 2005.

(3) (a) Mao, L.; Sakurai, H.; Hirao, T. *Synthesis* **2004**, 2535. (b) Eicher, T.; Hauptmann, S. *The Chemistry of Heterocycles*; Thieme: New York, 1995; pp 417−422 and 434.

(4) (a) Thomas, K. R. J.; Lin, J. T.; Tao, Y.-T.; Chuen, C. H. *J. Mater. Chem.* **2002**, *12*, 3516. (b) Chen, C.-T.; Lin, J.-S.; Moturn, M. V. R. K.; Lin, Y.-W.; Yi, W.; Tao, Y.-T.; Chien, C.-H. *Chem. Commun.* **2005**, 3980. (c) Thomas, K. R. J.; Velusamy, M.; Lin, J. T.; Chuen, C.-H.; Tao, Y.-T. *Chem. Mater.* **2005**, *17*, 1860. (d) Aldakov, D.; Palacios, M. A.; Anzenbacher, P., Jr. *Chem. Mater.* **2005**, *17*, 5238. (e) Chen, C.-T.; Wei, Y.; Lin, J.-S.; Motoru, M. V. R. K.; Chao, W.-S.; Tao, Y.-T.; Chien, C.-H. *J. Am. Chem. Soc.* **2006**, *128*, 10992.

(5) (a) Kulkarni, A. P.; Zhu, Y.; Babel, A.; Wu, P.-T.; Jenekhe, S. A. *Chem. Mater.* **2008**, *20*, 4212. (b) Xu, X.; Yu, G.; Chen, S.; Di, C.; Liu, Y. *J. Mater. Chem.* **2008**, *18*, 299. (c) Chen, S.; Xu, X.; Liu, Y.; Qiu, W.; Yu, G.; Wang, H.; Zhu, D. *J. Phys. Chem. C* **2007**, *111*, 1029. (d) Chen, S.; Xu, X.; Liu, Y.; Yu, G.; Sun, X.; Qiu, W.; Ma, Y.; Zhu, D. *Adv. Funct. Mater.* **2005**, *15*, 1541. (e) Kulkarni, A. P.; Zhu, Y.; Jenekhe, S. A. *Macromolecules* **2005**, *38*, 1553. (f) Zhao, L.; Perepichka, I. F.; Türksoy, F.; Batsanov, A. S.; Beeby, A.; Findlay, K. S.; Bryce, M. R. *New J. Chem.* **2004**, *28*, 912. (g) Thomas, K. R. J.; Lin, J. T.; Tao, Y.-T.; Chuen, C.-H. *Chem. Mater.* **2002**, *14*, 2796.

(6) (a) Kulkarni, A. P.; Tonzola, C. J.; Babel, A.; Jenekhe, S. A. *Chem. Mater.* **2004**, *16*, 4556. (b) Schmitz, C.; Pösch, P.; Thelakkat, M.; Schmidt, H.-W.; Montali, A.; Feldman, K.; Smith, P.; Weder, C. *Adv. Funct. Mater.* **2001**, *11*, 41. (c) Cui, Y.; Zhang, X.; Jenekhe, S. A. *Macromolecules* **1999**, *32*, 3824. (d) Redecker, M.; Bradley, D. C. C.; Jandke, M.; Strohriegl, P. *Appl. Phys. Lett.* **1999**, *75*, 109. (e) Jandke, M.; Strohriegl, P.; Berleb, S.; Werner, E.; Brütting, W. *Macromolecules* **1998**, *31*, 6434. (f) Fukuda, T.; Kanbara, T.; Yamamoto, T.; Ishikawa, K.; Takezoe, H.; Fukuda, A. *Appl. Phys. Lett.* **1996**, *68*, 2346. (g) O'Brien, D.; Weaver, M. S.; Lidzey, D. G.; Bradley, D. D. C. *Appl. Phys. Lett.* **1996**, *69*, 881.

(7) Son, H.-J.; Han, W.-S.; Wee, K.-R.; Yoo, D.-H.; Lee, J.-H.; Kwon, S.-N.; Ko, J.; Kang, S. O. *Org. Lett.* **2008**, *10*, 5401.

(8) Mancilha, F. S.; Neto, B. A. D.; Lopes, A. S.; Moreira, P. F., Jr.; Quina, F. H.; Gonçalves, R. S.; Dupont, J. *Eur. J. Org. Chem.* **2006**, 4924.

10.1021/jo9002147 CCC: $40.75 © 2009 American Chemical Society
Published on Web 03/23/2009

SCHEME 1. Synthesis of Panchromatic Quinoxaline Derivatives 2

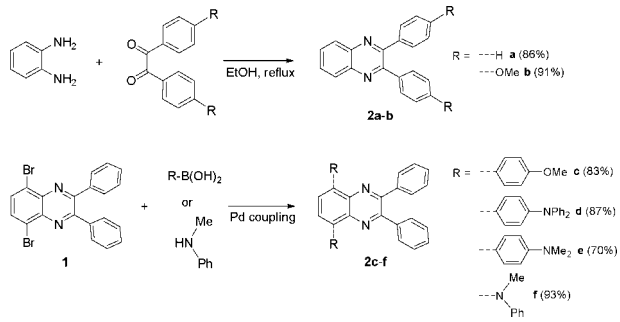

SCHEME 2. Synthesis of 2-Butylated Quinoxalines 3 Adjusted to Green Color

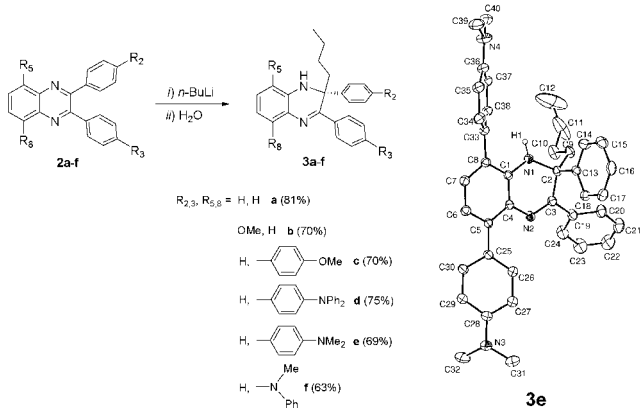

2 show the synthesis strategy for the synthesis of panchromatic quinoxaline derivatives **2** and corresponding quinoxaline derivatives **3** adjusted to green color, respectively.

The Pd-catalyzed C−C and C−N cross-coupling reactions of 5,8-dibromoquinoxaline (**1**) with suitable ED groups were performed successfully to yield the desired bipolar quinoxalines (**2c**−**f**). These included −OMe, $-NPh_2$, and $-NMe_2$ in the *para*-position of an aryl group or a direct substituted donor (−NMePh). A series of electronically modified 2-butylated quinoxalines (**3**) were synthesized in good yield (63−81%) from the reaction of **2** with *n*-butyllithium and subsequent hydrolysis. In all cases, the products were isolated by flash column chromatography. The production of **2** and subsequent 2-butylation at the "pyrazine" unit were identified by NMR spectroscopy (^{1}H and ^{13}C) and further confirmed by mass spectrometry and elemental analyses (see Experimental Section).

The geometrical change arising from the addition of a butyl group at the imine carbon atom of the pyrazine ring was confirmed by X-ray analyses of **3e**. As shown in Scheme 2 and Table S2 in Supporting Information, the typical tetrahedral geometry (110.3(2)−112.6(2)°) was verified by the four bond angles around the two-carbon center. The saturated N(1)−C(2) double bond (1.467(2) Å) by butyl and hydrogen groups produced a structural transformation from a trigonal planar to a bridge-headed tetrahedral geometry with an interrupted cyclic ring system, where one electron-accepting imine (sp^2-type) unit became an electron-donating amine (sp^3-type) (Figure S1 in Supporting Information).

Such a structural change on the pyrazine ring of **2** caused emission color tuning to green in **3**. Placement of successive ED groups around the EW quinoxaline ring created a panchromatic spectra of **2**, showing a broad range of both absorption

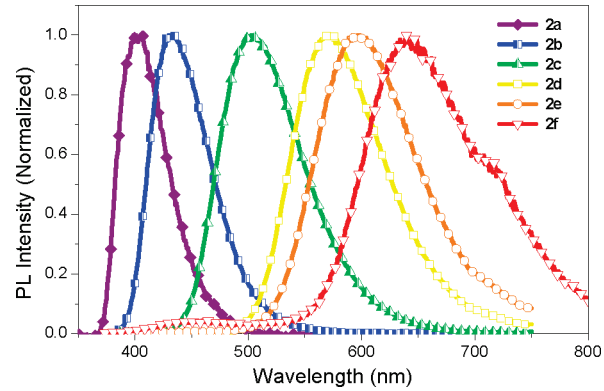

FIGURE 1. Panchromatic photoluminescence spectra of **2a**−**f**.

TABLE 1. Photophysical Properties of 2 and 3

		PL (λ_{max}/nm)			
sample	UV[a] (λ_{max}/nm)	solution[a]	film[b]	Stokes shift (cm^{-1})	Φ_f (%)[a]
2a	344	398	398	3945	*c*
2b	368	430	432	3919	18
2c	366	502	494	7403	57
2d	437	570	558	5340	51
2e	443	597	562	5824	30
2f	476	640	600	5384	1
3a	386	518	522	6603	60
3b	372	511	519	7313	52
3c	400	536	515	6344	45
3d	370	546	535	8713	27
3e	371	558	537	9034	16
3f	380	589	552	9339	1

[a] In chloroform. [b] Emission maximum for thin solid film. [c] It was difficult to measure this value due to the low intensity. All photoluminescent spectra were measured at each UV (λ_{max}/nm).

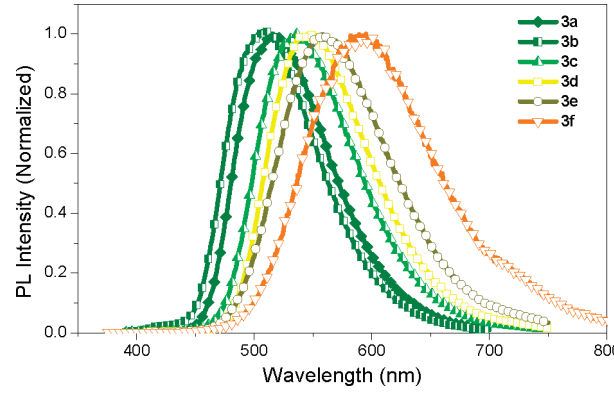

FIGURE 2. Reduced fluorescence range with a coherent green color emission spectra of **3** via C-alkylation.

(344−476 nm) and emission (398−640 nm), as shown in Figure 1 and Table 1. Due to the systematic electronic control originating from the ED−EW combinations, a large change in the Stokes shifts was observed for **2**. Upon 2-butylation, both absorption and emission appeared in a narrow spectral region, even with larger Stokes shifts (see Table 1). 2-Butylation altered the electronic structure of the quinoxalines to give a blue-shifted absorption and coherent green fluorescence. The quantum efficiencies of **3a**,**b** were higher than those of **2a**,**b**, while this trend was reversed in the **c**−**e** series, where the values of **2c**−**e** were larger than those in **3c**−**e** (Figure 2 and Table 1). It should be noted that the donor functionality of the aryl groups at the 2,3-position of quinoxalines appeared to be less effective in forming an ED−EW bipolar system with a pyrazine ring. The

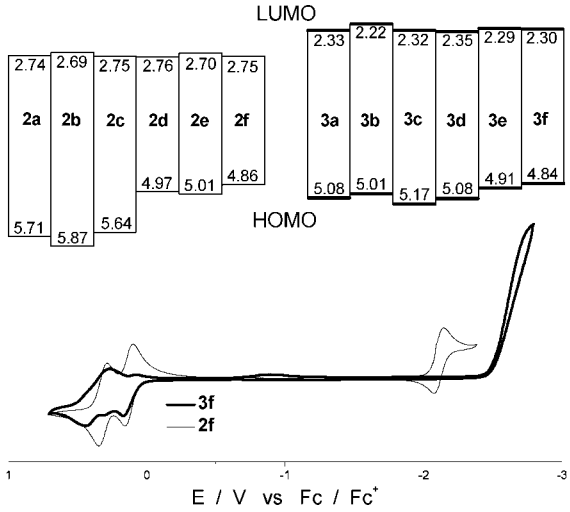

FIGURE 3. HOMO−LUMO levels of **2** and **3** obtained from CV data (top) and cyclic voltammograms of **2f** and **3f** (bottom).

silent fluorescence of **2a**,**b** was turned on by butylation at the imine carbon atom of the pyrazine ring, thereby creating ED amine functionality adjacent to the imine group to establish an efficient bipolar ED−EW system. On the other hand, the 5,8-positions were the most effective sites in electronic conjugation with the pyrazine ring. Therefore, highly luminescent bipolar ED−EW systems are indigenous to **2c**−**e**. Thus, the electronic systems for **3a**,**b** and **2c**−**e** appeared to be effective bipolar systems.

The electrochemical properties of the quinoxaline derivatives (**2**) and 2-alkylated compounds (**3**) were examined by cyclic voltammetry (CV). Figure 3 shows representative examples of compounds **2f** (shadowed) and **3f** (bold), where the most dramatic change was observed in the magnitude of the band gap (E_g^{el}) from 2.11 to 2.54 eV. **2f** exhibited characteristic bipolar characteristics due to the peripheral amine groups and electron-deficient imine units at the pyrazine ring, exhibiting reversible oxidation and reduction peaks at approximately 0.16−0.31 and −2.1 V, respectively. After C-alkylation at the imine units of the pyrazine ring (see Figure 3), as shown in the cyclic voltammogram of **3f**, notable features originated from the reduction wave and corresponding peak potential. The reversible reduction wave assigned to the imine nitrogen atom became irreversible, and the peak position was shifted to a much more negative potential of −2.7 V. Such a large shift in the reduction potential is the origin of the wide band gaps of **3**, leading to the green color control. The trend found in the CV data for **2f** and **3f** was general for the rest of the series for **2** and **3** and manifested the wide band gaps observed in **3** (see Supporting Information).

The HOMO and LUMO energy levels of **2** and **3** were estimated from the oxidation and reduction onset potential measured by cyclic voltammetry. As shown in Figure 3, the band gaps between the HOMO and LUMO levels of compounds **3** were larger than those found in **2**. These values were invariant regardless of the substituents used, conforming the constant green fluorescence. There appeared to be a constant LUMO energy level for **2** and **3**, while the HOMO energy levels of **2** varied considerably depending on the type of ED group used.

To address the origin of fluorescence control, a series of Dmol[3] DFT calculations[9] for **2** and **3** were carried out as shown in Supporting Information (Figure S7 and Table S5). Similar

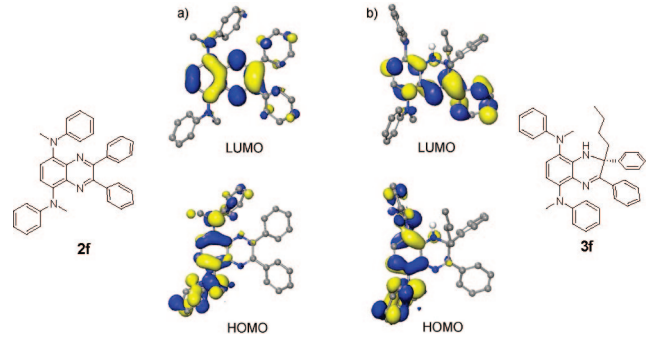

FIGURE 4. HOMO and LUMO diagrams of **2f** (a) and **3f** (b) obtained from Dmol[3] calculations.

to other ED−EA system,[10] distinctive contributions of each atomic orbital are discernible in the HOMO and LUMO diagrams of compounds **2** and **3**. As representative examples, panels a and b of Figure 4 show the HOMOs and LUMOs for **2f** and **3f**, respectively. There appears to be a regular trend in both the HOMO and LUMO for compound **2** (see Figure S7 in Supporting Information), where a 5,8-aryl or amino group with a fused benzene ring mainly contributes to the HOMO and an electron-deficient pyrazine ring always contributes to the LUMO. The LUMO energy levels are invariant because there are no overlapping orbitals attached to the benzopyrazine ring. However, 5,8-substituents effectively increased HOMO energy levels in the compound **2c**−**f** series with an increase in ED capability (see Figure S8 in Supporting Information). This observation is consistent to the bathochromic shift observed in the **2c**−**f** series (see Figure 1). In the case of **3** (see Figure S7 in Supporting Information), the HOMO diagrams consist mainly of 5,8-substituents and adorned fused benzene ring, while the LUMOs display a disrupted orbital distribution in the pyrazine moiety due to the presence of two different nitrogen atoms derived from 2-butylation. In particular, the LUMOs of **3** are significantly different from those found in **2**, possessing a large orbital contribution at the 3-position aryl substituent and benzopyrazine ring except for the butylated carbon atom at the 2-position. Such changes were attributed mainly to an increase in the energy levels of the LUMOs. Such a large change of LUMO distribution in **3** provides a reasonable explanation for the origin of fluorescent control by C-alkylation, namely, the wide band gap fluorescence.

In summary, panchromatic fluorescence materials (**2**) were developed by adopting a suitable donor substituent at the 5,8-positions of the quinoxalines. Subsequently, quinoxaline compounds (**2**) were readily converted into new types of bipolar ED−EA compounds, 2-butylated quinoxaline (**3**), by selective C-alkylation at the 2-position. A coherent green fluorescence centered at approximately 550 nm was observed as a result of the controlled electron density caused by the geometrical change. The CV and theoretical data corroborated the electronic control in **2** to **3**. Using this unique method, studies of practical applications for a colorimetric indicator of any quinoxaline moiety are currently underway.

Experimental Section

Compound 3c. A 2.5 M solution of *n*-BuLi (0.44 mL, 1.1 mmol) in hexane was added to a stirred THF solution (15 mL) of 2,3-

(9) (a) Delley, B. *J. Chem. Phys.* **1990**, *92*, 508. (b) Delley, B. *J. Chem. Phys.* **2000**, *113*, 7756.

(10) Kulkarni, A. P.; Wu, P.-T.; Kwon, T. W.; Jenekhe, S. A. *J. Phys. Chem. B* **2005**, *109*, 19584.

diphenyl-5,8-bis(4-methoxyphenyl)quinoxaline (**2c**) (0.494 g, 1 mmol) at −78 °C. The resulting mixture was then warmed to room temperature and stirred for 3 h. The mixture was hydrolyzed with water. The organic layer was extracted with CH_2Cl_2 and dried over magnesium sulfate. The solvent was removed under reduced pressure, and the residue was purified by silica gel column chromatography using ethyl acetate/hexane (1:20) as the eluent. **3c** was obtained as a green powder (0.387 g, 70%): mp 156−157 °C; ^{1}H NMR ($CDCl_3$) δ 7.63 (d, 2H), 7.47 (d, 2H), 7.40 (d, 2H), 7.34 (t, 2H), 7.29−7.13 (m, 6H), 7.01−6.93 (m, 5H), 6.84 (d, 1H), 4.28 (s, 1H), 3.85 (s, 3H), 3.84 (s, 3H), 2.41 (t, 1H), 1.96 (t, 1H), 1.64−1.51 (m, 1H), 1.27−1.12 (m, 3H), 0.71 (t, 3H); ^{13}C NMR ($CDCl_3$) δ 160.1, 159.0, 158.8, 145.2, 138.7, 138.3, 133.5, 132.3, 131.9, 130.6, 130.2, 129.7, 128.9, 128.8, 128.7, 127.8, 127.6, 126.5, 124.7, 119.0, 114.7, 113.1, 61.0, 55.4, 55.4, 37.7, 26.7, 23.0, 13.9; HRMS(FAB) calcd for $C_{38}H_{36}N_2O_2$ 552.2777, found 552.2786 $[M]^+$. Anal. Calcd for $C_{38}H_{36}N_2O_2$: C, 82.58; H, 6.57; N, 5.07. Found: C, 82.37; H, 6.47; N, 5.04.

Acknowledgment. This work was supported by the Korea Science and Engineering Foundation (KOSEF) NRL program grant funded by the Korea government (MEST) (No. R0A-2008-000-20090-0) and ERC Program (No. R11-2008-088-02002-0).

Supporting Information Available: Experimental details and characterization data, CIF, related optical data, CVs, and calculation data. This material is available free of charge via the Internet at http://pubs.acs.org.

JO9002147